Classification
Physics Abstracts
68.00 — 05.20

Monte Carlo study of the inflation-deflation transition in a fluid membrane

B. Dammann ([1]), H. C. Fogedby ([2]), J. H. Ipsen ([1]) and C. Jeppesen ([3])

([1]) Department of Physical Chemistry, The Technical University of Denmark, DK-2800 Lyngby, Denmark
([2]) Institute of Physics and Astronomy, University of Aarhus, DK-8000 Aarhus C, Denmark
([3]) Materials Research Laboratory, University of California, Santa Barbara, CA 93106, U.S.A.

(*Received 22 February 1994, accepted 15 April 1994*)

Abstract. — We study the conformation and scaling properties of a self-avoiding fluid membrane, subject to an osmotic pressure p, by means of Monte Carlo simulations. Using finite size scaling methods in combination with a histogram reweighting techniques we find that the surface undergoes an abrupt conformational transition at a critical pressure p^*, from low pressure deflated configurations with a branched polymer characteristics to a high pressure inflated phase, in agreement with previous findings [1, 2]. The transition pressure p^* scales with the system size as $p^* \propto N^{-\alpha}$ with $\alpha = 0.69 \pm 0.01$. Below p^* the enclosed volume scales as $V \propto N$, in accordance with the self-avoiding branched polymer structure, and for $p \searrow p^*$ our data are consistent with the finite size scaling form $V \propto N^{\beta_+}$, where $\beta_+ = 1.43 \pm 0.04$. Also the finite size scaling behavior of the radii of gyration and the compressibility moduli are obtained. Some of the observed exponents and the mechanism behind the conformational collapse are interpreted in terms of a Flory theory.

1. Introduction.

Over the past several years there has been an increased interest in the phase behavior and morphological properties of flexible, fluid interfaces. Beside the theoretical challenge in understanding surfaces as two dimensional generalizations of polymers, they are expected to be of relevance in physical systems ranging from simple interfaces between coexisting fluids close to the consolute point to surfactant interfaces in e.g. microemulsions and lipid membranes [4-7].

In the context of modelling lipid vesicles it is of particular importance to study the conformation of closed membranes in the presence of surface tension, bending rigidity, osmotic pressure between the interior and the exterior of the membrane, etc. For a simple, closed, fluid membrane with bending rigidity $\kappa \cdot k_B T$, pressure $p \cdot k_B T$ and fixed overall

topology, the vesicle conformation is determined by the energy functional,

$$H/k_B T = \frac{\kappa}{2} \int dA \left(\frac{1}{R_1} + \frac{1}{R_2} \right)^2 - p \int dV , \quad (1)$$

where R_1 and R_2 are the principal radii of curvature [8]. This phenomenological form is the basis for detailed descriptions of shape transformations of rigid vesicles with $\kappa \gg 1$ [9, 10]. There is a general consensus that sufficiently large, unconstrained fluid self-avoiding surfaces collapse into branched polymer-like structures with the characteristics of branched polymers for $T > 0$ [11]. This general feature will not be changed by e.g., the presence of bending stiffness. However, the osmotic pressure difference between the interior and exterior of a closed surface is a quantity of direct experimental relevance, which is expected to change this situation.

The properties of two-dimensional vesicles (ring-polymers), subject to a pressure p controlling the enclosed volume (area), have been explored in a number of studies [12-21] Leibler, Singh and Fisher [12] verified by numerical studies that 2-D flexible vesicles change continuously from a deflated state with characteristics of branched polymers to an inflated state as p is increased. This change is accompanied by crossovers in scaling exponents characterizing the surface. The scaling-behavior of the inflated regime can be interpreted in terms of Pincus stretching exponents for polymers [14, 30]. Real-space-RG studies of a lattice model equivalent to the 2-D vesicle problem [20] and exact configurational enumeration techniques [16] show agreement with the numerical studies. The universal relations have also been confirmed by use of conformal techniques on the lattice model [18]. Furthermore, analytical studies of pressurized, flexible, but self-intersecting surfaces in 2-D have been carried out [21]. Only few studies have been carried out in 3-D. In [22, 23] pressurized, flexible, fluid surfaces have been considered in the context of the confined phases of some lattice gauge models. These studies have focussed on the effect of pressure on vesicle topology for deflated vesicles.

It has recently been demonstrated by numerical studies that pressurized, flexible surfaces in 3-D undergo a first-order-like transition from a deflated phase with branched polymer behavior to inflated configurations. Gompper and Kroll based their studies on a triangulated random surface model [1], while Baumgärtner applied a plaquette model for a self-avoiding surface [2, 3], where the surface is composed of the domain walls of a spin-model. In these studies the basic scaling relations, established for 2-D flexible, pressurized surfaces, were generalized to three dimensions.

In the present paper we also consider a fluid membrane with an osmotic pressure p, but with zero bending rigidity κ. Its properties are analyzed on the basis of computer simulations of a triangulated random surface representation of the fluid membrane. Using the Ferrenberg-Swendsen reweighting techniques [25] we attempt a precise determination of the critical pressure and the scaling exponents in the deflated and inflated phases.

2. Model.

The model considered here is a simple extension of the Ho-Baumgärtner description of self-avoiding surfaces [27]. It consists of a closed triangular network of beads positioned at the N vertices of the network with the topology of a sphere. To each vertex position $\mathbf{X}_i$ is associated a bead with hard core diameter 1. In order to enforce the self-avoidance constraint the length of the flexible tether between neighboring vertices is chosen to be less than $\sqrt{2}$. The fluidity of the surface is modelled by a dynamical change of the connectivity between the vertices by means of « flip » transformations which correspond to deleting a tether or link between

neighboring vertices and attempting to form a new link between the adjacent vertices in the two triangles involved. Finally, the shape changes are generated by a local updating of the vertex position, the « shift » transformation, $\mathbf{X}_i \to \mathbf{X}_i + \delta\mathbf{X}_i$, where $\delta\mathbf{X}_i$ represent an incremental change in the local surface position. $\delta\mathbf{X}_i$ is picked randomly within a cube, where the cube-side is adjusted to preserve self-avoidance. These procedures ensure sampling over all possible self-avoiding, piece-wise linear surfaces consisting of N beads and with the topology of a sphere. The updating of the surface shapes is posed by standard Monte Carlo techniques [28] on the partition function

$$Z = \sum_{\text{Surface shapes}} \exp(-H/k_B T) . \tag{2}$$

In the simulations a discretized version of the Hamiltonian from equation (1) with $\kappa = 0$ is applied. In order to obtain a fast updating rate a dynamic sublattice structure is implemented which keeps track of the N vertices during shape transformations. We furthermore use data structures consisting of linked lists which, given an arbitrary vertex or link, allow an identification of the adjacent triangles. The last feature implies an oriented triangulation and leads to the following expressions for the area of the surface and the enclosed volume :

$$A = \sum_n \Delta A_n = \frac{1}{2} \sum_{ij\ell} \left| (\mathbf{X}_i - \mathbf{X}_j) \times (\mathbf{X}_\ell - \mathbf{X}_j) \right| , \tag{3}$$

and

$$V = \sum_n \Delta V_n = \frac{1}{6} \sum_{ij\ell} \mathbf{X}_i \cdot (\mathbf{X}_j \times \mathbf{X}_\ell) . \tag{4}$$

The indices $ij\ell$ pertain to the corners of an oriented triangle and the sum runs over all triangles of the triangulation.

Using a stress ensemble we have collected data for a range of p values and N values (N is the number of vertices). In a simulation we typically measure the following quantities :

- we monitor the shift and flip rates in order to ensure a suitable balance between fluidity (the flip rate) and shape changes (the shift rate),
- for the characterization of the over-all membrane size we sample the radius of gyration R_G :

$$R_G^2 = \frac{1}{N} \sum_{i=1}^{N} (\mathbf{X}_i - \mathbf{X}_{CM})^2 , \tag{5}$$

where $\mathbf{X}_{CM} = \frac{1}{N} \sum_{i=1}^{N} \mathbf{X}_i$ is the center of mass,

- the area A and the volume V of the membrane are monitored.

The measured quantities are stored for construction of probability distributions and evaluation of equilibrium thermal averages. It is characteristic of fluctuating membrane systems that the correlations times are quite long and grow fast with the system size. Careful analysis of the time series is thus very important to ensure proper equilibrium sampling of the fluctuating surface. E.g., for $N = 400$ we sample 20 Mill MCS/vertex in order to equilibrate the system and perform measurements over about 400 Mill MCS/vertex. We have investigated system sizes ranging from $N = 49$ to $N = 400$.

3. Simulations and data analysis.

The Ferrenberg-Swendsen reweighting of the probability distributions allow for an approximate determination of thermal averages for a pressure value p close to the simulation pressure p_0, if the phase space is properly sampled, e.g. for the averaged volume $\langle V \rangle$ it takes the form :

$$\langle V \rangle_p = \frac{\sum_i V_i P(V_i) \exp(-\Delta p V_i)}{\sum_i P(V_i) \exp(-\Delta p V_i)} , \tag{6}$$

where $\Delta p = p - p_0$, and $P(V_i)$ is the sampled distribution. The sum is running over all measured volume values. Figure 1 shows the averaged vesicle volume *versus* pressure p for two different system system sizes $N = 100$ and 196, obtained from simulations at different pressures. The lines are the results of the reweighting technique, using only one simulation near the assumed critical pressure. The dramatic change in the vesicle volume over a narrow pressure interval indicates the presence of a phase transition in the thermodynamic limit $N \to \infty$ from a low pressure deflated phase to a high pressure inflated phase in accordance with the simulations of Gompper and Kroll [1] The plots of volume *versus* pressure thus allow an approximate determination of the critical pressure p^* The reweighting technique also enables us to reconstruct the phase diagram. In the insert of figure 1 we show the reconstructed volume *versus* pressure curves for $N = 81$, 100, 121, 144, 169, 196, 225, 256, 324, 400 obtained by use of equation (6).

A more precise determination of the critical pressure can be obtained by evaluating the total volume fluctuations $\langle V^2 \rangle - \langle V \rangle^2$ and estimate the peak position. Figure 2 shows the

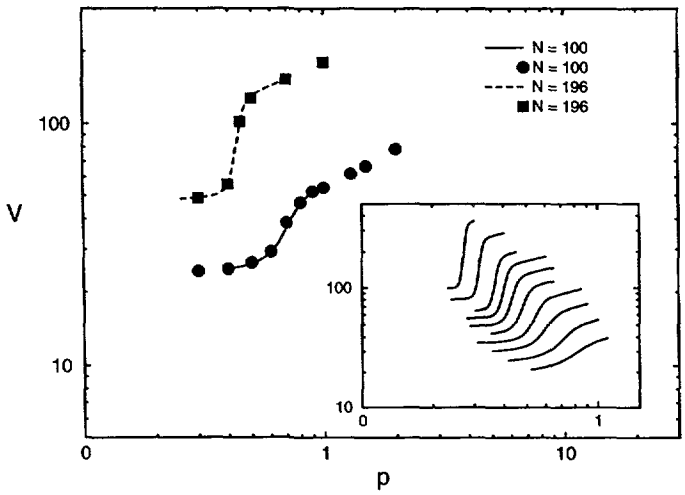

Fig. 1. — In this figure the volume averages $\langle V \rangle$ obtained from simulations at different pressures are plotted *vs.* p, for two different system sizes ($N = 100$ and $N = 196$). The lines are the results from the Ferrenberg-Swendsen reweighting for a single simulation at $p = 0.7$ for $N = 100$ and $p = 0.445$ for $N = 196$. The insert shows the volume values obtained with the Ferrenberg-Swendsen reweighting technique from simulations near the critical pressure, for $N = 81$, 100, 121, 144, 169, 196, 225, 256, 324, 400.

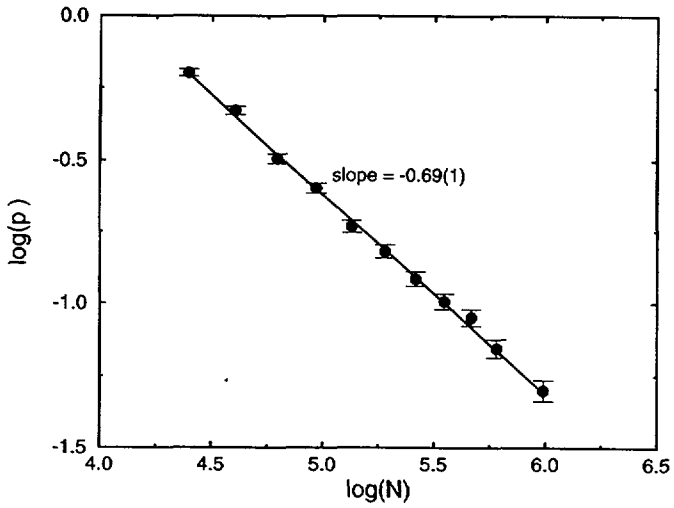

Fig. 2. — This figure shows log (p^*) *vs.* log (N). The values for p^* are obtained from the peak in the total compressibility $\langle(\Delta V)^2\rangle$, which was calculated using the Ferrenberg-Swendsen reweighting technique. The exponent is obtained from fitting to -0.69 ± 0.01.

measured p^* for different system sizes. p^* is well described by a power-law in N :

$$p^* \sim N^{-\alpha} \tag{7}$$

where $\alpha = 0.69 \pm 0.01$, obtained from a linear fit to the double-logarithmic representation of the data. All indicated error bars are related to the regression analysis.

The Ferrenberg-Swendsen reweighting technique [25] can also be applied for the construction of the probability distribution $P(V)$ at specific pressures near the anticipated critical pressure p^*. In figure 3 we show examples of measured histograms representing $P(V)$ and $P(R_G^2)$ for $N = 144$ at $p = 0.52$ and $p = 0.54$. The measured $P(V)$ at $p = 0.52$ is in good agreement with the probability distribution obtained from reweighting the histogram measured at $p = 0.54$. At p^*, $P(V)$ has a characteristic double-peak structure representing the two phases. Lee and Kosterlitz used this technique to determine finite-size transition points for lattice models by matching the peak-heights, and by investigation of their finite-size behavior information about the nature of the transition in the thermodynamic limit can be obtained [26]. It is a key assumption in this procedure that the probability distribution for some density can be well described as the superposition of Gaussian distributions. This is not fulfilled for $P(V)$, but some properties of the distribution will be considered. $P(V)$ can in a first approximation be written as the superposition of contributions from inflated and deflated contributions :

$$P(V) \simeq a_- P_-(V) + a_+ P_+(V), \tag{8}$$

as suggested by e.g. figure 3. The maximum probability volumes for the two peaks V_- and V_+ can easily be estimated and is shown in figure 4. We find the dependence :

$$V_\pm \sim N^{\beta_\pm}, \tag{9}$$

where the associated scaling exponents are $\beta_- = 0.99 \pm 0.01$ and $\beta_+ = 1\ 43 \pm 0.04$.

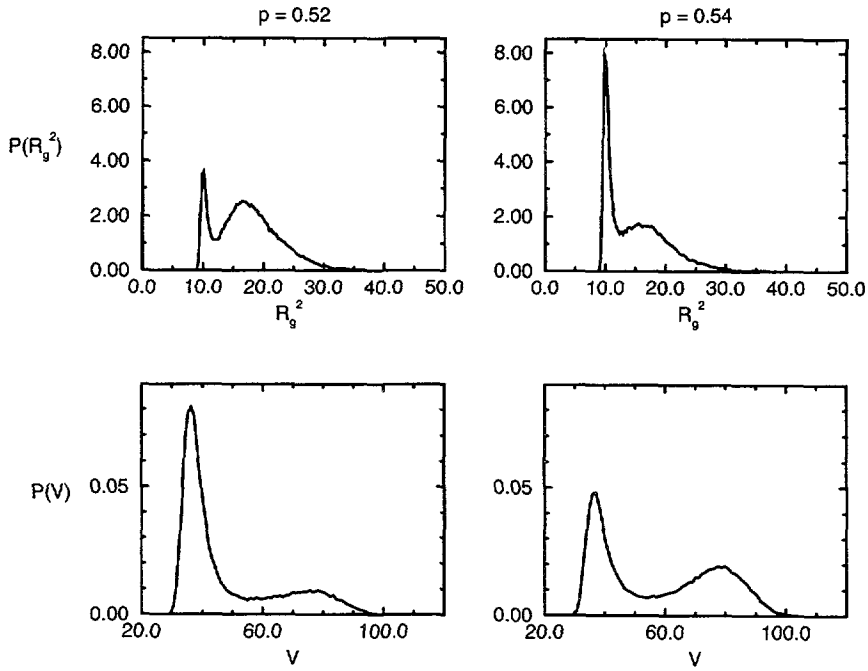

Fig. 3. — The distributions $P(V)$ and $P(R_G^2)$ are plotted for two different pressure values and the system size $N = 144$. The sharp peak in the $P(R_G^2)$ distribution belongs to the inflated phase, whereas the corresponding peak in the $P(V)$ distribution is broader. For the branched polymer configuration it is opposite.

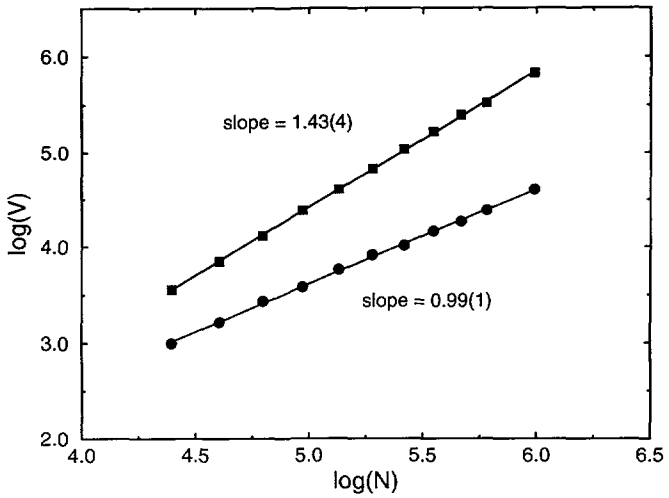

Fig. 4. — The volumes V_- and V_+ corresponding to the two peaks in $P(V)$ at p^* are plotted against N in a double logarithmic representation. The regression lines correspond to $V_\pm \propto N^{\beta_\pm}$ where $\beta_- = 0.99 \pm 0.01$ and $\beta_+ = 1.43 \pm 0.04$.

Since the two peaks in $P(V)$ display very different dependences of N, P_- and P_+ have been analyzed separately. In figure 5 P_+ is given in a double logarithmic representation up to a multiplicative factor. The plot indicates that the volume distribution for the inflated phase of the surface has a universal form for large N.

$$P_+(V) \simeq \frac{1}{N^{\beta_+}} f_+ \left(\frac{V}{N^{\beta_+}} \right), \tag{10}$$

where f_+ is represented in figure 5 as the limiting distribution as N becomes large. Our data are not sufficient for a thorough analysis of the form of f_+.

The probability distribution describing the volume fluctuations of the deflated configurations are given in the insert of figure 5. Similar to P_+, P_- approach a universal form as N becomes large :

$$P_-(V) \simeq f_-(V - V_-), \tag{11}$$

f_- is represented in the insert. The volume fluctuations $\langle (\Delta V)^2 \rangle_-$ are thus independent of N.

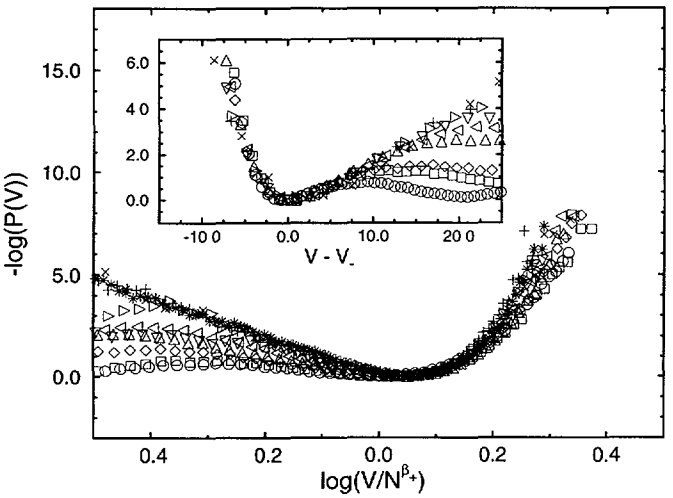

Fig. 5. — The unnormalized volume probability distributions at p^* for N = 100, 121, 144, 169, 196, 225, 256, 324, 400. $P(V)$ is for each N multiplied by a common factor so the maxima are equal unity. P_+, the part of the histograms associated with the inflated configurations is plotted against V/N^{β_+} in a log-log representation. P in the insert is the low-volume parts of the histograms representing the inflated configurations similarly given in a semi-logarithmic plot.

At p^* the probability distribution for the radius of gyration R_G^2 displays a double-peak similar to the probability distribution of the volume, as shown in figure 3. The peak-positions are identified with the radii of gyration of the inflated and the deflated phases $R_\pm^2$. The calculated $R_\pm^2$ shown in figure 6 indicate a relationship :

$$R_\pm^2 \sim N^{2\nu_\pm}, \tag{12}$$

where $2\nu_- = 1.05 \pm 0.05$ and $2\nu_+ = 0.81 \pm 0.01$.

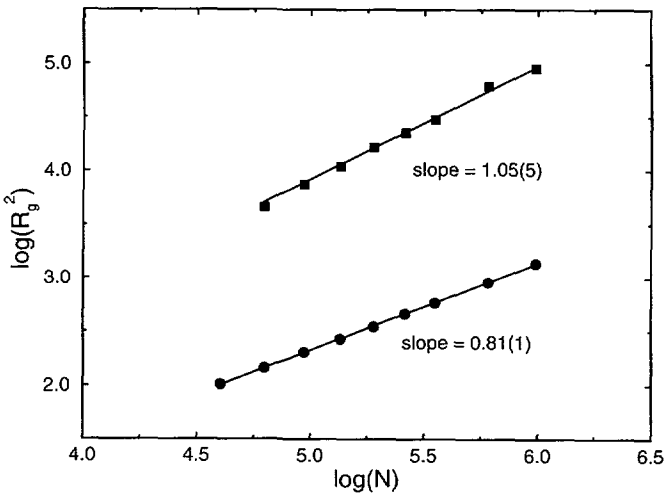

Fig. 6. — The radii of gyration R_-^2 and R_+^2 at p^* are plotted against N. The data are indicative of a relationship $R_\pm^2 \propto N^{\nu_\pm}$ where $\nu_- = 1.05 \pm 0.05$ and $\nu_+ = 0.81 \pm 0.01$.

In figure 7 the data for the total volume fluctuations $K = \langle V^2 \rangle - \langle V \rangle^2$ at p^* is plotted against N. From the regression analysis in the log-log representation we obtain a dependence :

$$K(p^*) \sim N^\gamma , \tag{13}$$

where $\gamma = 3.62 \pm 0.02$.

4. Discussion and conclusion.

The above analysis confirms that fluid, flexible vesicles undergo an abrupt conformational change between a deflated and an inflated regime at some small pressure value which

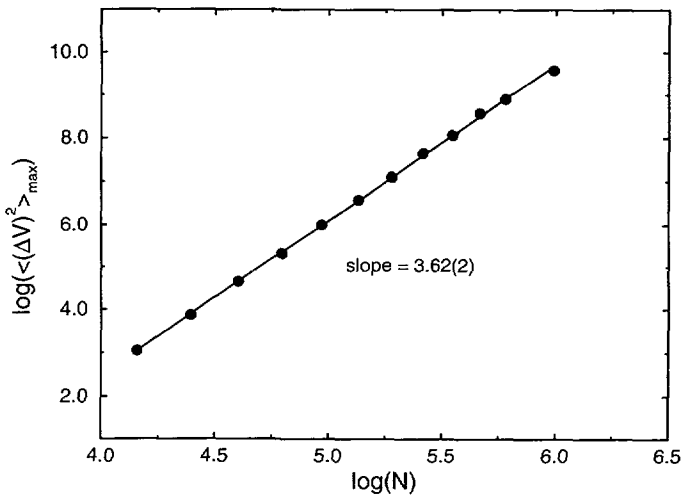

Fig. 7. — The maximum of the total volume fluctuations $\langle (\Delta V)^2 \rangle = \langle V^2 \rangle - \langle V \rangle^2$ (corresponding to p^*) is plotted vs N in a log-log representation. The fit indicates $\langle (\Delta V)^2 \rangle_{max} \sim N^\gamma$, with $\gamma = 3.62 \pm 0.02$.

diminishes with the system size according to a power-law, $p^* \propto N^{-\alpha}$, where $\alpha = 0.69 \pm 0.01$. The value of this exponent is in disagreement with previous findings 0.5 [1] and 1 [2].

In the deflated regime $p < p^*$ the data are consistent with branched polymer configurations of the surface :

$$\langle V \rangle_- \propto \langle R_G^2 \rangle_- \propto N , \tag{14}$$

and thus support the general expectation that unpressurized, fluid membrane conformations are controlled by the branched polymer fixed point, i.e. the stable $\kappa = 0$ crumpling fixed point [1, 29].

In the inflated phase for $p > p^*$, generalizing Pincus' result for polymer stretching [30], Gompper and Kroll [1] and Baumgärtner [2] propose the scaling form

$$\begin{aligned} \langle R_G^2 \rangle_+ &\sim p^{2(2\bar{\nu}-1)} N^{2\bar{\nu}} \\ \langle V \rangle_+ &\sim p^{3(2\bar{\nu}-1)} N^{3\bar{\nu}} , \end{aligned} \tag{15}$$

where $\bar{\nu}$ is a new scaling exponent characterizing the stretched phase. In the following we will use the short notation $R = \sqrt{\langle R_G^2 \rangle_+}$.

At the critical pressure inserting the scaling result $p^* \sim N^{-\alpha}$ in equation (15), we obtain for $\langle V \rangle_+$ in the inflated phase,

$$\langle V \rangle_+ \sim N^{3[\bar{\nu} - \alpha(2\bar{\nu}-1)]} , \tag{16}$$

and we derive the relationship $\beta_+ = 3[\bar{\nu} - \alpha(2\bar{\nu} - 1)]$. From the numerically obtained exponents $\beta_+ \simeq 1.43$ and $\alpha \simeq 0.69$ in equations (9) and (7) we find $\bar{\nu} \simeq 0.56$ which is in a reasonable agreement with Gompper and Kroll [1] ($\bar{\nu} = 7/12 = 0.583$). However, a similar analysis of R_G^2 leads to a significantly different estimate $\bar{\nu} \simeq 0.75$.

Another consequence of equation (15) is, that for $p \searrow p^*$:

$$\frac{\langle (\Delta V)^2 \rangle_+}{\langle V \rangle_+} = \frac{1}{\langle V \rangle_+} \frac{\partial \langle V \rangle_+}{\partial p} \sim (p^*)^{-1} \sim N^{\alpha} , \tag{17}$$

which is contradictory to the numerical finding $\langle (\Delta V)^2 \rangle_+ / \langle V \rangle_+ \sim N^{\beta_+}$, where $\langle (\Delta V)^2 \rangle_+ \sim N^{2\beta_+}$ at the transition is a consequence of equation (10). Finally, we find $\langle V \rangle_+ / R^3 \propto N^{\beta_+ - 3\nu_+}$, where $\beta_+ - 3\nu_+ \simeq 0.22$ at the transition, so the relation $\langle V \rangle_+ \propto R^3$ is not consistent with our data. The numerical data, obtained in the transition region, are not sufficient for an extended scaling analysis, however, with the above considerations we conclude that they do not support an ansatz of the type (15).

In the following we will discuss the inflation-deflation collapse transition of a fluid surface within the framework of a Flory theory which has been applied to the description of polymeric, flexible surfaces [32] and attempted applied in the context of plaquette surfaces [33]. The application of sufficient pressure will restrict the configurational phase space and prevent branching of the surface. Such a surface can for « small » pressures allow an effective description in terms of a Flory theory for the free energy :

$$F_1 = \frac{R^2}{R_0^2} + v \frac{N^2}{R^d} - p\gamma NR . \tag{18}$$

The first two terms represent the standard Flory theory for a surface, where R_0 is the radius of gyration for a self-intersecting surface, $R_0 \sim N^{\nu_0}$, where $\nu_0 = 0$, and v is the excluded volume parameter. $d = 3$ is the dimension of the embedding space. In the last term the pressure couples to the volume :

$$\langle V \rangle_+ \propto \left\langle \int_A d\mathbf{A}\mathbf{n} \cdot (\mathbf{X} - \mathbf{X}_{CM}) \right\rangle_+ \propto \langle \cos\theta \rangle_+ \cdot NR , \tag{19}$$

where $\theta = \angle (\mathbf{X} - \mathbf{X}_{CM}, \mathbf{n})$ and $\mathbf{n}$ is the surface normal at surface position $\mathbf{X}$. Here it is used that $|\mathbf{X} - \mathbf{X}_{CM}|$ is distributed around R in the inflated configurations, so equation (19) represents the leading contribution to $\langle V \rangle_+$. The parameter γ in equation (18) is thus proportional to $\langle \cos\theta \rangle_+ > 0$. The stationary condition for F_1 at $p = 0$ can be characterized by a critical exponent ν:

$$R \propto N^{\nu} , \qquad \nu = \frac{2}{d+2} = \frac{2}{5} = 0.4 ,$$

$$\langle V \rangle_+ \propto NR \propto N^{\beta} , \qquad \beta = 1 + \nu = \frac{7}{5} = 1\,4 . \tag{20}$$

These Flory exponents are indeed close to the numerically obtained $\nu_+ = 0.41$ and $\beta_+ = 1.43$. But since $F_1 \propto N^{2\nu}$, these configurations are unstable with respect to branched polymer collapse for large N and F_1 must be considered as a metastable free-energy branch for $p = 0$. The branched polymer configurations are completely entropy dominated with an approximate free energy [1 11] .

$$F_{bp} = -\ln(z^*) N + \frac{3}{2} \ln(N) - pN , \tag{21}$$

where $z^* > 1$. Let us now apply a small pressure, so that the relations in equations (20) still hold. The characteristic pressure p^* separating the unstable $p = 0$ region from the inflated region in F_1 is given by $p^* N^{1+\nu} \sim N^{2\nu}$ leading to $p^* \propto N^{-\bar{\alpha}}$, where $\bar{\alpha} = 1 - \nu = 3/5 = 0.6$. For a choice of $\bar{\alpha}$ smaller than 3/5 the perturbative considerations break down and the pressure term will dominate in equation (18), which eventually leads to complete inflation with $F \propto -pN^{3/2}$ for $N \to \infty$. For $\bar{\alpha}$ larger than 3/5 the surface will be controlled by the $p = 0$ behavior as N becomes large. This simple analysis thus suggests that the trigger of the inflation-deflation transition can be understood on basis of the cross-over from the flaccid to the inflated conformations of closed, flexible, polymeric surfaces under pressure. The strong fluctuations in the transition region, e.g. observed in the probability distributions, are not included in this consideration. In particular it must be expected that fluctuations in the weakly inflated regime will modify the conditions for the stability of the inflated configurations. The deviation of $\bar{\alpha}$ from the numerically obtained exponent $\alpha = 0.69$ is thus not surprising in light of the crudeness of the approximations involved.

In the present paper we have reanalyzed the deflation-inflation transition of a fluid membrane subject to an inflating pressure discovered by Gompper and Kroll [1], and Baumgärtner [2]. In the transition region we find low-pressure configurations with the characteristics of branched polymers and an exponent for the radius of gyration $\nu_- = \nu_{BP} = 0.52 \pm 0.03$ and high pressure configurations, with a characteristic exponent $\nu_- = 0.41 \pm 0.01$. Analysis of the volume distribution functions show that the two phases display universal properties at p^*, characterized by exponents for the volume $\beta_- = 0.99 \pm 0.01$ and $\beta_\perp = 1\,43 \pm 0.04$ for the two types of configurations in the transition region.

Further, a simple analysis of the transition within the framework of Flory theory accounts for some of the observed exponents and suggests a mechanism for the transition. The exponents characterizing the finite-size behavior of the transition pressure and the total volume fluctuations are subjects to further investigations.

Acknowledgments.

We would like to thank Ole G. Mouritsen and Martin J. Zuckermann for illuminating discussions. We also wish to thank Benny Lautrup for permission to run some of the simulations on his workstation.

References

[1] Gompper G. and Kroll D. M., *Europhys. Lett.* **19** (1992) 581 *Phys. Rev. A* **46** (1992) 7466.
[2] Baumgärtner A., *Physica A* **190** (1992) 63.
[3] Baumgärtner A., *J. Chem. Phys.* **98** (1993) 7496.
[4] Physics of Amphiphilic Layers, J. Meunier, D. Langevin and N. Boccara Eds. (Springer-Verlag, Berlin 1987).
[5] Statistical Mechanics of Membranes and Surfaces, D. R. Nelson, T. Piran and S. Weinberg (World Scientific, Singapore, 1989).
[6] International Workshop on Geometry and Interfaces, E. Dubois-Violette and B. Pansu Eds., *J. Phys. Colloq. France* **51** (1990) C7.
[7] de Gennes P. G. and Taupin C., *J. Phys. Chem.* **86** (1982) 2294.
[8] Helfrich W., *Z Naturforsch.* **28c** (1973) 693.
[9] Deuling H. J. and Helfrich W., *J. Phys. France* **37** (1976) 1335.
[10] Miao L., Fourcade B., Rao M., Wortis M. and Zia R. K. P., *Phys. Rev. A* **43** (1991) 6843.
[11] Durhuus B., Frölich J. and Jonsson T., *Nucl. Phys.* **B 225** (1983) 185.
[12] Leibler S., Singh R. R. P. and Fisher M. E., *Phys. Rev. Lett.* **59** (1987) 1989.
[13] Camacho C. J. and Fisher M. E., *Phys. Rev. Lett.* **65** (1990) 9.
[14] Maggs A. C., Leibler S., Fisher M. E. and Camacho C. J., *Phys. Rev. A* **42** (1990) 691.
[15] Camacho C. J. and Fisher M. E., *J. Chem. Phys.* **94** (1991) 5693.
[16] Fisher M. E., Guttmann A. J. and Whittington S. G., *J. Phys. A* **24** (1991) 3095.
[17] Morikawa R. and Saito Y., *J. Phys. II France* **4** (1994) 145.
[18] Cardy J., Preprint cond-mat@babbage.sissa.trieste.it/9310013.
[19] Romero A., *J. Phys. I France* **2** (1992) 15.
[20] Banavar J. R., Maritan A. and Stella A., *Phys. Rev A* **43** (1991) 5752.
[21] Gaspari G., Rudnick J. and Fauver M., *J. Phys. A* **26** (1993) 15.
[22] Banavar J. R., Maritan A. and Stella A., *Science* **252** (1991) 825.
[23] Stella A., *Physica A* **185** (1992) 211.
[24] A. L. Stella, Orlandini E., Beichl I Sullivan F., Tesi M. C. and Einstein T. L., *Phys. Rev. Lett* **69** (1992) 3650.
[25] Ferrenberg A. M. and Swendsen R. H., *Phys. Rev. Lett.* **61** (1988) 2635.
[26] Lee J. and Kosterlitz J. M., *Phys. Rev Lett* **65** (1990) 137 ; *Phys. Rev.* **B 43** (1991) 3265.
[27] Baumgärtner A. and Ho J.-S., *Phys. Rev. A* **41** (1990) 5747 ; *Europhys Lett.* **12** (1990) 295.
[28] Mouritsen O. G., Computer Studies of Phase Transitions and Critical Phenomena (Springer-Verlag, Heidelberg, 1984).
[29] Boal D. H. and Rao M., *Phys. Rev. A* **45** (1992) R6947.
[30] Pincus P., *Macromolecules* **9** (1976) 386.
[31] de Gennes P. C., Scaling Concepts in Polymer Physics (Cornell University Press, Ithaca, N.Y., 1979).
[32] Kantor Y., Kardar M. and Nelson D. R., *Phys Rev. A* **35** (1987) 3056.
[33] Maritan A. and Stella A., *Phys. Rev. Lett.* **53** (1984) 123.